Hybrid Position/Force Adaptive Control of Redundantly Actuated Parallel Manipulators[1)]

SHEN Hui[1] WU Xu-Zhong[1] LIU Guan-Feng[2] LI Ze-Xiang[2]
[1](*College of Mechatronical Engineering & Automation, National University of Defense Technology, Changsha* 410073, *P. R. China*)
(E-mail: xzwu@nudt. edu. cn)
[2](*Department of Electrical and Electronic Engineering, Hong Kong University of Science and Technology, Hongkong, P. R. China*)
(E-mail: manifold_nudt@163. com)

Abstract An adaptive hybrid position/force control approach for redundantly actuated parallel manipulators is presented. Based on the geometric properties of constraint submanifolds in parallel manipulators, the inverse dynamics of redundantly actuated parallel manipulators can be naturally projected to configuration subspace and constraint force subspace. Based on the projection equations, a unified and asymptotically stable adaptive hybrid position/force control algorithm is proposed. With the minimal two-norm rule, the redundancy resolution problem is solved and the practical actuated forces are optimized. Simulation results are given to demonstrate the effectiveness of the proposed approach.

Key words Redundant actuation, parallel robots, adaptive control, hybrid control

1 Introduction

Force and velocity in constrained systems are objects of different physical and geometric nature, where constraint forces annihilate free velocities. The duality relation between force and velocity has been applied to designing hybrid position/force controllers[1]. For instance, Yoshikawa presented a dynamic hybrid position/force control algorithm[2]. McClamroch explicitly utilized the duality relation and the constraints to decouple the dynamics of the constrained mechanical systems and developed a stable hybrid position/force control algorithm[3]. Selig also used the duality relation to define two projection maps and gave a precise geometric interpretation of the constrained dynamics[4].

In this paper, we study geometric properties of constraint submanifolds of parallel manipulators and provide a unified geometric framework for modeling and control of them. Using the metric and the constraint, we define two projection maps. By them, we decompose the Euler-Lagrange equation of the parallel manipulator into two orthogonal components. Subsequently, we design an adaptive hybrid position/force controller for the planar two-degree-of-freedom parallel manipulator with redundant actuators described in [5] and theoretical analysis and simulation results validate its asymptotically stability. The proposed method has some attractive features: First, by decoupling the inverse dynamics, we can design respectively controllers for different control performance. Second, by an adaptive control law, robustness to parametric uncertainty is achieved. Finally, the controller designing and redundant actuated forces optimization are considered separately, and the control algorithm is not complicated and is suitable for practical applications.

2 Geometry of the constraint systems

A holonomic constraint mechanical system can be modeled as follows

1) Supported by National Netural Science Foundation of P. R. China(50029501)
Received May 8, 2002; in revised form September 16, 2002
收稿日期 2002-05-08; 收修改稿日期 2002-09-16

$$H:E \to R^{n-m}, \quad H(\theta) = (h_1(\theta), \cdots, h_{n-m}(\theta))^{\mathrm{T}} = 0 \tag{1}$$

By excluding singularities, the configuration space $Q=H^{-1}(0)$ of the constraint system is m-dimension embedded submanifold in E which is called generalized coordinate space of the constrained system[6]. At each $\theta \in Q$, the tangent space of Q, $T_\theta Q$, defines the set of free velocities of the constrained system, which is the free velocity space. Utilizing the duality relation between free velocities and constraint forces, the constraint force space is defined by

$$T^{\cdot} Q^{\perp} = \{ f \in T_\theta^{\cdot} E \mid \langle f, v \rangle = 0, \forall v \in T_\theta Q \} \tag{2}$$

where $\langle f, v \rangle$ denotes the virtual work produced by generalized forces f acting on generalized velocity v.

Let $T=\frac{1}{2}\dot{\boldsymbol{\theta}}^{\mathrm{T}} M(\boldsymbol{\theta})\dot{\boldsymbol{\theta}}$ be the kinetic energy of the mechanical system. It endows $T_\theta E$ with a natural Riemannian metric M. Using this metric, the orthogonal complement of $T_\theta Q$ can be defined as

$$T_\theta Q^{\perp} = \{ v_1 \in T_\theta E \mid \langle\langle v_1, v_2 \rangle\rangle_M = v_1^{\mathrm{T}} M v_2 = 0, \forall v_2 \in T_\theta Q \} \tag{3}$$

and the cotangent space $T^{\cdot} Q$ consists of covectors which annihilate vectors in $T_\theta Q^{\perp}$

$$T_\theta^{\cdot} Q = \{ f \in T_\theta^{\cdot} E \mid \langle f, v \rangle = 0, \forall v \in T_\theta Q^{\perp} \} \tag{4}$$

The above discussion shows that a holonomically constrained system is naturally associated with two subspaces $T_\theta Q^{\perp}$ and $T_\theta^{\cdot} Q$. If the system is further endowed with a kinetic energy metric M, and then two additional subspaces $T_\theta Q^{\perp}$ and $T_\theta^{\cdot} Q$ can be defined. These subspaces have obvious relations with generalized velocity space and generalized force space as follows

$$T_\theta E = T_\theta Q \oplus T_\theta Q^{\perp} \quad T_\theta^{\cdot} E = T_\theta^{\cdot} Q \oplus T_\theta^{\cdot} Q^{\perp} \tag{5}$$

Using the metric M, we can define the mapping

$$M^b : T_\theta E \to T_\theta^* E: \quad \langle M^b v1, v2 \rangle = v_1^{\mathrm{T}} M v_2 \quad v_1, v_2 \in T_\theta E \tag{6}$$

As M is positive definite, M^b has an inverse, denoted by M^χ. It is not difficult to see that the matrix representation of M^b is simply M and that of M^χ is M^{-1}. In addition, these mappings satisfy

$$M^\chi(T_\theta^* Q) = T_\theta Q \quad M^\chi(T_\theta^* Q^{\perp}) = T_\theta Q^{\perp} \tag{7}$$

From (1), we get the push forward mapping and pull back mapping of H respectively as follows:

$$H_* : T_\theta E \to T_{H(\theta)} R^{n-m} \quad H^* : T_{H(\theta)}^* R^{n-m} \to T_\theta^* E \tag{8}$$

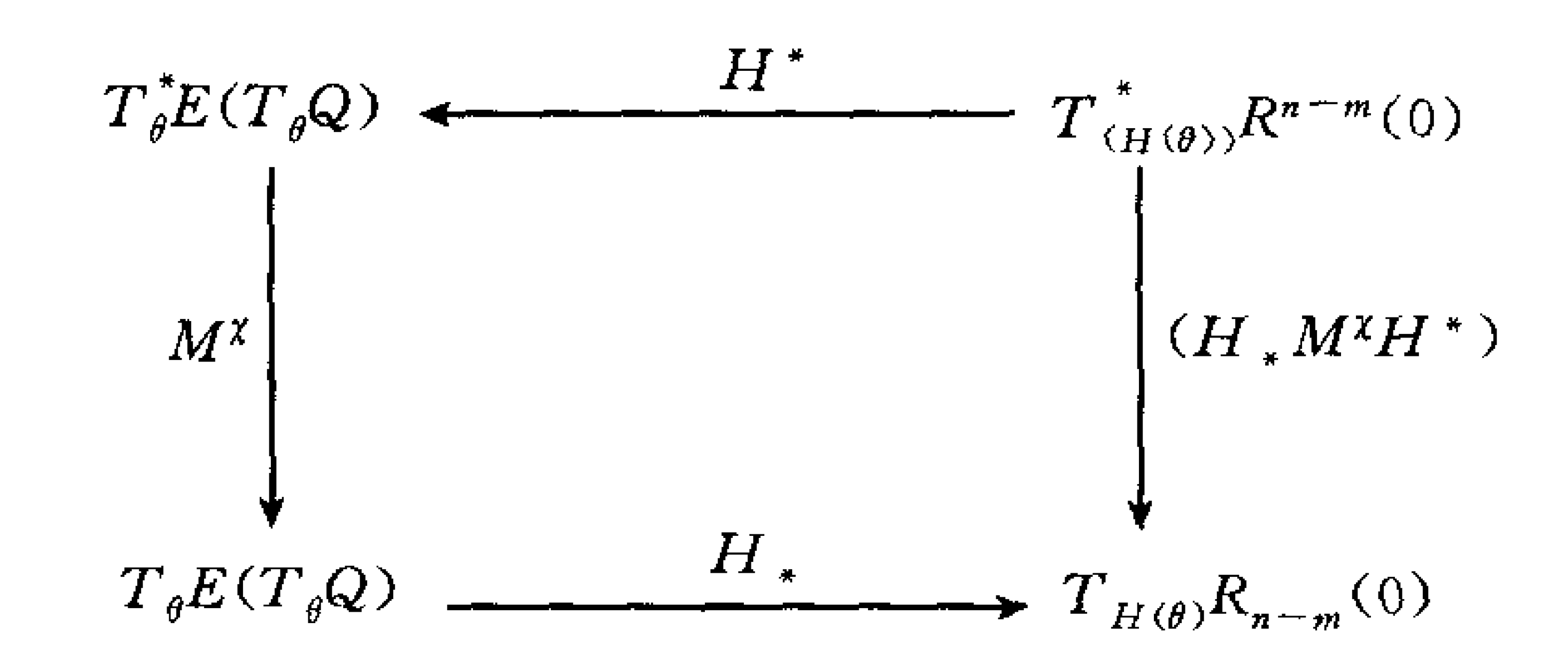

Fig. 1 Commutative diagram for different subspaces

It is obvious that the null space of H_* satisfies $N(H_*)=T_\theta Q$. Thus, H_* identifies $T_\theta Q^{\perp}$ with $T_{H(\theta)} R^{n-m}$ and H^* identifies $T_{H(\theta)}^* R^{n-m}$ with $T_\theta^* Q^{\perp}$. Figure 1 shows the commutative diagram for these subspaces.

Lemma 1. Assume mapping $I-P_\omega$ is given by

$$I - P_\omega = H^* (H_* M^\chi H^*)^{-1} H_* M^\chi \tag{9}$$

Then mappings $I-P_\omega$ and P_ω are the projection mappings from $T^* E$ to $T_\theta^* Q^{\perp}$ and $T_\theta^* Q$, respectively.

Proof. Given $f_1 \in T_\theta^* Q$, we have $M^\chi(f_1) \in T_\theta Q = N(H_*)$, and $(I-P_\omega)(f_1)=0$. On the other hand, for $f_2 \in T_\theta^* Q^{\perp}$, there exists $\lambda \in R^{n-m}$ such that $f_2 = H^* \lambda$ and

$$(I - P_\omega) f_2 = H^* (H_* M^\chi H^*)^{-1} H_* M^\chi H_* M^\chi H^* \lambda = H^* \lambda = f_2$$

This shows that $I-P_\omega$ is the projection mapping from $T^* E$ to $T_\theta^* Q^{\perp}$. In a similar manner, we know that mapping P_ω is the projection mapping to $T_\theta^* Q$.

For a parallel mechanical system, the inverse dynamics equations are written[1] by

$$\boldsymbol{M}\ddot{\boldsymbol{\theta}} + \boldsymbol{C}(\boldsymbol{\theta},\dot{\boldsymbol{\theta}})\,\dot{\boldsymbol{\theta}} + \boldsymbol{N} = \boldsymbol{\tau} + \boldsymbol{A}^{\tau}\boldsymbol{\lambda} \tag{10}$$

where $\boldsymbol{M}$ denotes the inertia matrix , $\boldsymbol{C}$ centrifugal and Coriolis forces and $\boldsymbol{N}$ the gravitational force. The Lagrange multipliers $\boldsymbol{\lambda}$ represent the magnitude of constraint forces, whose directions are defined by $\boldsymbol{A} = \partial H/\partial \boldsymbol{\theta}^{\mathrm{T}}$.

Differentiating the constraint equation (1) and eliminating second differential terms from (10) we have

$$\boldsymbol{\lambda} = (\boldsymbol{A}\boldsymbol{M}^{-1}\boldsymbol{A}^{\mathrm{T}})^{-1}(-\dot{\boldsymbol{A}}\dot{\boldsymbol{\theta}} + \boldsymbol{A}\boldsymbol{M}^{-1}(\boldsymbol{C}\dot{\boldsymbol{\theta}} + \boldsymbol{N} - \boldsymbol{\tau})) \tag{11}$$

Substituting (11) back to (10) yields

$$\boldsymbol{M}\ddot{\boldsymbol{\theta}} + \boldsymbol{A}^{\mathrm{T}}(\boldsymbol{A}\boldsymbol{M}^{-1}\boldsymbol{A}^{\mathrm{T}})^{-1}\dot{\boldsymbol{A}}\dot{\boldsymbol{\theta}} + P_{\omega}\boldsymbol{C}\dot{\boldsymbol{\theta}} + P_{\omega}\boldsymbol{N} = P_{\omega}\boldsymbol{\tau} \tag{12}$$

where

$$P_{\omega} = \boldsymbol{I} - \boldsymbol{A}^{\mathrm{T}}(\boldsymbol{A}\boldsymbol{M}^{-1}\boldsymbol{A}^{\mathrm{T}})^{-1}\boldsymbol{A}\boldsymbol{M}^{-1} \tag{13}$$

Thus, we write the dynamics equation (11) in a simple form

$$\boldsymbol{M}\ddot{\boldsymbol{\theta}} + \boldsymbol{A}^{\mathrm{T}}(\boldsymbol{A}\boldsymbol{M}^{-1}\boldsymbol{A}^{\mathrm{T}})^{-1}\dot{\boldsymbol{A}}\dot{\boldsymbol{\theta}} = P_{\omega}\boldsymbol{M}\ddot{\boldsymbol{\theta}} \overset{\mathrm{def}}{=} \overline{\boldsymbol{M}}\ddot{\boldsymbol{\theta}} \tag{14}$$

Defining $\overline{\boldsymbol{C}} = P_{\omega}\boldsymbol{C}$, $\overline{\boldsymbol{N}} = P_{\omega}\boldsymbol{N}$ and $\bar{\boldsymbol{\tau}} = P_{\omega}\boldsymbol{\tau}$, we have

$$\overline{\boldsymbol{M}}\ddot{\boldsymbol{\theta}} + \overline{\boldsymbol{C}}(\boldsymbol{\theta},\dot{\boldsymbol{\theta}})\dot{\boldsymbol{\theta}} + \overline{\boldsymbol{N}} = \bar{\boldsymbol{\tau}} \tag{15}$$

Comparing equations (15) and (10), It is obvious that the right hand side of (15) does not include the constraint forces term. That is by the projection mapping $P_{\omega}: T^{*}E \rightarrow T^{*}Q$, the inverse dynamics of the parallel manipulator is projected to the cotangent space of its configuration space. Defining $H_{*} = \boldsymbol{A}, H^{*} = \boldsymbol{A}^{\tau}, M^{b} = \boldsymbol{M}, M^{\chi} = \boldsymbol{M}^{-1}$, it is seen that (13) is consistent with the equation (9). In order to project the dynamics to the constraint force space, constituting another project mapping $(I - P_{\omega}): T^{*}E \rightarrow T^{*}Q^{\perp}$ according to (9), we have

$$(\boldsymbol{I} - P_{\omega})(\boldsymbol{M}\ddot{\boldsymbol{\theta}} + \boldsymbol{C}\dot{\boldsymbol{\theta}} + \boldsymbol{N}) = (\boldsymbol{I} - P_{\omega})\boldsymbol{\tau} + \boldsymbol{A}^{\mathrm{T}}\boldsymbol{\lambda} \tag{16}$$

To summarize, we decouple the dynamics of parallel mechanical systems to position space and constraint force space respectively by (15) and (16). □

3 Adaptive hybrid control algorithm

Considering the planar two-degree-of-freedom parallel manipulator shown in Figure 2. We denote actuated joints $\tilde{\boldsymbol{\theta}} = [\theta_1, \theta_2]^{\tau}$, the redundant actuated joint θ_3, and the generalized coordinates $\boldsymbol{\theta} = [\theta_1, \phi_1, \theta_2, \phi_2, \theta_3, \phi_3]$. Let $\boldsymbol{\theta} = \psi(\tilde{\boldsymbol{\theta}})$ be the embedded mapping from Q to E, and $\boldsymbol{J}$ the corresponding Jacobian matrix, we have

$$\dot{\boldsymbol{\theta}} = \boldsymbol{J}\dot{\tilde{\boldsymbol{\theta}}} \quad \ddot{\boldsymbol{\theta}} = \boldsymbol{J}\ddot{\tilde{\boldsymbol{\theta}}} + \dot{\boldsymbol{J}}\dot{\tilde{\boldsymbol{\theta}}} \tag{17}$$

Substituting (17) to (10) yields

$$\boldsymbol{M}\boldsymbol{J}\ddot{\tilde{\boldsymbol{\theta}}} + \boldsymbol{M}\dot{\boldsymbol{J}}\dot{\tilde{\boldsymbol{\theta}}} + \boldsymbol{C}(\psi(\tilde{\boldsymbol{\theta}}), \boldsymbol{J}\dot{\tilde{\boldsymbol{\theta}}})\boldsymbol{J}\dot{\tilde{\boldsymbol{\theta}}} + \boldsymbol{N} = \boldsymbol{\tau} + \boldsymbol{A}^{\mathrm{T}}\boldsymbol{\lambda} \tag{18}$$

According to the previous discussion, we have the decoupled dynamics by the project mapping P_{ω} as follows

$$P_{\omega}\boldsymbol{M}\boldsymbol{J}\ddot{\tilde{\boldsymbol{\theta}}} + P_{\omega}(\boldsymbol{C}_1\dot{\tilde{\boldsymbol{\theta}}} + \boldsymbol{N}) = P_{\omega}\boldsymbol{\tau} \tag{19}$$

$$(\boldsymbol{I} - P_{\omega})\boldsymbol{M}\boldsymbol{J}\ddot{\tilde{\boldsymbol{\theta}}} + (\boldsymbol{I} - P_{\omega})(\boldsymbol{C}_1\dot{\tilde{\boldsymbol{\theta}}} + \boldsymbol{N}) = (\boldsymbol{I} - P_{\omega})\boldsymbol{\tau} + \boldsymbol{A}^{\mathrm{T}}\boldsymbol{\lambda} \tag{20}$$

where $\boldsymbol{C}_1(\tilde{\boldsymbol{\theta}}, \dot{\tilde{\boldsymbol{\theta}}}) = \boldsymbol{C}(\psi(\tilde{\boldsymbol{\theta}}), \boldsymbol{J}\dot{\tilde{\boldsymbol{\theta}}})\boldsymbol{J} + \boldsymbol{M}\dot{\boldsymbol{J}}$.

Lemma 2[7]. Let $\overline{\boldsymbol{M}} = \boldsymbol{J}^{\mathrm{T}}\boldsymbol{M}\boldsymbol{J}$ and $\overline{\boldsymbol{C}}_1 = \boldsymbol{J}^{\mathrm{T}}\boldsymbol{C}_1$. We have

1) The matrix $\overline{\boldsymbol{M}}$ is symmetric, positive definite, and both $\overline{\boldsymbol{M}}$ and $\overline{\boldsymbol{M}}^{-1}$ are uniformly bounded functions.

2) The matrix $\dot{\overline{\boldsymbol{M}}} - 2\overline{\boldsymbol{C}}_1$ is skew symmetric.

Define the sliding surface as follows[7]

$$\boldsymbol{r} = \tilde{\boldsymbol{\theta}} - \boldsymbol{v} - \boldsymbol{\Lambda}_2 \boldsymbol{e}_f = \dot{\boldsymbol{e}}_m + \boldsymbol{\Lambda}_1 \boldsymbol{e}_m - \boldsymbol{\Lambda}_2 \boldsymbol{e}_f \tag{21}$$

where $\boldsymbol{v}=\tilde{\boldsymbol{\theta}}_d - \boldsymbol{\Lambda}_1 \boldsymbol{e}_m$, $\boldsymbol{e}_m = \tilde{\boldsymbol{\theta}} - \tilde{\boldsymbol{\theta}}_d$, $\dot{\boldsymbol{e}}_f = \boldsymbol{A}_f \boldsymbol{e}_f + \boldsymbol{A}^{\mathrm{T}}\boldsymbol{\lambda} - \boldsymbol{f}_d$ and $\boldsymbol{e}_f(0) = \boldsymbol{e}_{f_0}$. $\tilde{\boldsymbol{\theta}}_d$ and $\boldsymbol{f}_d$ represent the desired trajectory of motion and constraint forces, respectively. Λ_1 and Λ_2 are tunable positive definite matrices and A_f is a stable matrix. The adaptive controller consists of a motion control law and a force control law given by

$$P_\omega \boldsymbol{\tau} = \hat{\boldsymbol{M}}\boldsymbol{J}\dot{\boldsymbol{v}} + \hat{\boldsymbol{C}}_1 \boldsymbol{v} + \frac{1}{2}\hat{\boldsymbol{N}} - \boldsymbol{J}^{-T}\boldsymbol{k}_d \boldsymbol{r} \tag{22}$$

$$(\boldsymbol{I} - P_\omega)\boldsymbol{\tau} = (\hat{\boldsymbol{M}}\boldsymbol{J}\boldsymbol{\Lambda}_2 - \boldsymbol{I}_{6\times 6})\,\dot{\boldsymbol{e}}_f + (\hat{\boldsymbol{C}}_1 \boldsymbol{\Lambda}_2 + \boldsymbol{A}_f)\boldsymbol{e}_f + \frac{1}{2}\hat{\boldsymbol{N}} - \boldsymbol{f}_d \tag{23}$$

where $\boldsymbol{k}_d$ is a tunable diagonal gain matrix and $\hat{\boldsymbol{M}}$, $\hat{\boldsymbol{C}}$ and $\hat{\boldsymbol{N}}$ are the estimates of corresponding matrices respectively. Substitute the above equations back to (18), and we have

$$\boldsymbol{M}\boldsymbol{J}\ddot{\tilde{\boldsymbol{\theta}}} + \boldsymbol{C}_1 \dot{\tilde{\boldsymbol{\theta}}} + \boldsymbol{N} = \hat{\boldsymbol{M}}\boldsymbol{J}\dot{\boldsymbol{v}} + \hat{\boldsymbol{C}}_1 \boldsymbol{v} + \hat{\boldsymbol{N}} - \boldsymbol{k}_d \boldsymbol{r} + \hat{\boldsymbol{M}}\boldsymbol{J}\boldsymbol{\Lambda}_2\, \dot{\boldsymbol{e}}_f + \hat{\boldsymbol{C}}_1 \boldsymbol{\Lambda}_2 \boldsymbol{e}_f \tag{24}$$

Let
$$\boldsymbol{M}_f = (\boldsymbol{M}\boldsymbol{J}\dot{\boldsymbol{v}} + \boldsymbol{C}_1 \boldsymbol{v} + \boldsymbol{N} - \boldsymbol{k}_d \boldsymbol{r}) + (\boldsymbol{M}\boldsymbol{J}\boldsymbol{\Lambda}_2 \dot{\boldsymbol{e}}_f + \boldsymbol{C}_1 \boldsymbol{\Lambda}_2 \boldsymbol{e}_f) \tag{25}$$

and eliminate $\boldsymbol{M}_f$ from the both sides of (24), rewrite (24) as

$$\boldsymbol{M}\boldsymbol{J}\dot{\boldsymbol{r}} + \boldsymbol{C}_1 \boldsymbol{r} + \boldsymbol{J}^{-T}\boldsymbol{k}_d \boldsymbol{r} = (\hat{\boldsymbol{M}} - \boldsymbol{M})(\boldsymbol{J}\dot{\boldsymbol{v}} + \boldsymbol{\Lambda}_2 \dot{\boldsymbol{e}}_f) + (\hat{\boldsymbol{C}}_1 - \boldsymbol{C})(\boldsymbol{v} + \boldsymbol{\Lambda}_2 \boldsymbol{e}_f) + (\hat{\boldsymbol{N}} - \boldsymbol{N}) =$$

$$\boldsymbol{Y}(\tilde{\boldsymbol{\theta}}, \dot{\tilde{\boldsymbol{\theta}}}, \tilde{\boldsymbol{\theta}}_d, \dot{\tilde{\boldsymbol{\theta}}}_d, \boldsymbol{v}, \dot{\boldsymbol{v}}, \boldsymbol{e}_f, \dot{\boldsymbol{e}}_f)\tilde{\boldsymbol{p}} \tag{26}$$

where $\tilde{\boldsymbol{p}} = \hat{\boldsymbol{p}} - \boldsymbol{p}$. Multiply both sides of the above equation by $\boldsymbol{J}^{\mathrm{T}}$ and let $\bar{\boldsymbol{Y}} = \boldsymbol{J}^{\mathrm{T}}\boldsymbol{Y}$. We have

$$\bar{\boldsymbol{M}}\dot{\boldsymbol{r}} + \bar{\boldsymbol{C}}_1 \boldsymbol{r} + \boldsymbol{k}_d \boldsymbol{r} = \bar{\boldsymbol{Y}}(\tilde{\boldsymbol{\theta}}, \dot{\tilde{\boldsymbol{\theta}}}, \tilde{\boldsymbol{\theta}}_d, \dot{\tilde{\boldsymbol{\theta}}}_d, \boldsymbol{v}, \dot{\boldsymbol{v}}, \boldsymbol{e}_f, \dot{\boldsymbol{e}}_f)\tilde{\boldsymbol{p}} \tag{27}$$

The parameter adaptation law is chosen as

$$\dot{\hat{\boldsymbol{p}}} = -\boldsymbol{\Gamma}^{-1}\bar{\boldsymbol{Y}}^{\mathrm{T}}\boldsymbol{r} \tag{28}$$

where $\boldsymbol{\Gamma}$ is a symmetric gain matrix.

Theorem 1. Consider the parallel manipulator described by (18). Using the control laws (22)-(23) and the parameter adaptation law (28), the closed-loop system is asymptotically stable.

Proof. Consider a Lyapunov function candidate

$$V = \frac{1}{2}\boldsymbol{r}^{\mathrm{T}}\bar{\boldsymbol{M}}\boldsymbol{r} + \frac{1}{2}\tilde{\boldsymbol{p}}^{\mathrm{T}}\boldsymbol{\Gamma}\tilde{\boldsymbol{p}} + \frac{1}{2}\boldsymbol{e}_m^{\mathrm{T}}\boldsymbol{P}_1 \boldsymbol{e}_m + \frac{1}{2}\boldsymbol{e}_f^{\mathrm{T}}\boldsymbol{P}_2 \boldsymbol{e}_f \tag{29}$$

where $\boldsymbol{P}_1$ and $\boldsymbol{P}_2$ satisfy the following equations, respectively,

$$\boldsymbol{P}_1 \boldsymbol{\Lambda}_1 + \boldsymbol{\Lambda}_1^{\mathrm{T}} \boldsymbol{P}_1 = \boldsymbol{Q}_1 \tag{30}$$

$$\boldsymbol{P}_2 \boldsymbol{A}_f + \boldsymbol{A}_f^{\mathrm{T}} \boldsymbol{P}_2 = -\boldsymbol{Q}_2 \tag{31}$$

In (30) and (31), $\boldsymbol{Q}_1$ and $\boldsymbol{Q}_2$ are positive-definite matrices. Differentiating (29) and according to Lemma 2 we have

$$\dot{V} = -\boldsymbol{r}^{\mathrm{T}}\boldsymbol{k}_d \boldsymbol{r} - \frac{1}{2}\boldsymbol{e}_m^{\mathrm{T}}\boldsymbol{Q}_1 \boldsymbol{e}_m + \boldsymbol{e}_m^{\mathrm{T}}\boldsymbol{P}_1 \boldsymbol{\Lambda}_2 \boldsymbol{e}_f + \boldsymbol{e}_m^{\mathrm{T}}\boldsymbol{P}_1 \boldsymbol{r} - \frac{1}{2}\boldsymbol{e}_f^{\mathrm{T}}\boldsymbol{Q}_2 \boldsymbol{e}_f + \boldsymbol{e}_f^{\mathrm{T}}\boldsymbol{P}_2(\boldsymbol{A}^{\mathrm{T}}\boldsymbol{\lambda} - \boldsymbol{f}_d) \tag{32}$$

We denote the stiffness matrix of the parallel manipulator by $\boldsymbol{K}$, and the constraint forces are just strain forces produced due to the departure from the equilibrium position of the end-effector, which are given by

$$\boldsymbol{f} = \boldsymbol{A}^{\mathrm{T}}\boldsymbol{\lambda} = \boldsymbol{K}(\boldsymbol{\theta} - \boldsymbol{\theta}_e) \tag{33}$$

Thus, we have $\|\boldsymbol{f}(\boldsymbol{\theta}) - \boldsymbol{f}_d(\boldsymbol{\theta}_d)\| = \|\boldsymbol{J}^{-T}\boldsymbol{K}(\tilde{\boldsymbol{\theta}} - \tilde{\boldsymbol{\theta}}_e) - \boldsymbol{J}^{-T}\boldsymbol{K}(\tilde{\boldsymbol{\theta}}_d - \tilde{\boldsymbol{\theta}}_e)\| \leqslant \|\boldsymbol{J}^{-T}\boldsymbol{K}\|\,\|\tilde{\boldsymbol{\theta}} - \tilde{\boldsymbol{\theta}}_d\| = \|\boldsymbol{J}^{-T}\boldsymbol{K}\|\,\|\boldsymbol{e}_m\|$.

Let $a_1 = \lambda_{\min}(\boldsymbol{k}_d)$, $a_2 = \lambda_{\min}\left(\frac{1}{2}\boldsymbol{Q}_1\right)$, $a_3 = \lambda_{\min}\left(\frac{1}{2}\boldsymbol{Q}_2\right)$ and $b_1 = \|\boldsymbol{P}_1\|$, $b_2 = \|\boldsymbol{P}_1 \Lambda_2\| + \|\boldsymbol{J}^{-T}\boldsymbol{K}\|\,\|\boldsymbol{P}_2\|$. We rewrite the (33) as

$$\dot{v} = -a_1\|\boldsymbol{r}\|^2 - a_2\|\boldsymbol{e}_m\|^2 - a_3\|\boldsymbol{e}_f\|^2 + b_1\|\boldsymbol{r}\|\,\|\boldsymbol{e}_m\| + b_2\|\boldsymbol{e}_m\|\,\|\boldsymbol{e}_f\| \tag{34}$$

According to [9], if $\boldsymbol{Q}_1$ and $\boldsymbol{Q}_2$ are properly chosen, we can assure that $\dot{v}$ is negative semi-definite. Therefore, the theorem holds. □

4 Optimization of redundantly actuated forces

From (22) and (23), we get the actuated forces in $T_\theta^* Q \in R^2$. In order to obtain each real actuated force, we need project these forces from $T_\theta^* Q \in R^2$ to $J_a \in R^3$. Due to existing of redundant actuators, this projection mapping is not unique, so these forces must be distributed onto each actuator of the manipulator according to some optimization rules.

Let
$$\tilde{\boldsymbol{\tau}} = (\tau_1, \tau_3, \tau_5)^{\mathrm{T}} \in R^{3\times 1}, \hat{\boldsymbol{P}}_\omega = [p_1, p_3, p_5] \in R^{6\times 3} \tag{35}$$
where $p_i, i=1,3,5$ is the ith column of P_ω. We have
$$\hat{\boldsymbol{\tau}} = \hat{\boldsymbol{P}}_\omega \tilde{\boldsymbol{\tau}} = \boldsymbol{P}_\omega \boldsymbol{\tau} \in T_\theta^* Q \tag{36}$$
Assume $\tilde{\boldsymbol{\tau}}_0 \in N(\hat{\boldsymbol{P}}_\omega)$ and $\tilde{\boldsymbol{\tau}}_1$ is a solution such that $\hat{\boldsymbol{P}}_\omega \tilde{\boldsymbol{\tau}}_1 = \hat{\boldsymbol{\tau}}$. Then actuated forces are given by
$$\tilde{\boldsymbol{\tau}} = \tilde{\boldsymbol{\tau}}_1 + \gamma \tilde{\boldsymbol{\tau}}_0 \tag{37}$$
Solve the following optimization problem
$$\min_{\gamma \in R} \| \tilde{\boldsymbol{\tau}}_1 + \gamma \tilde{\boldsymbol{\tau}}_0 \|_2 \tag{38}$$
and we get the optimal solution when $\gamma = -\dfrac{\langle \tilde{\boldsymbol{\tau}}_0, \tilde{\boldsymbol{\tau}}_1 \rangle}{\langle \tilde{\boldsymbol{\tau}}_0, \tilde{\boldsymbol{\tau}}_0 \rangle}$. Thus we have realized minimal torque position control on the planar 2-DOF parallel manipulator shown in Figure 2.

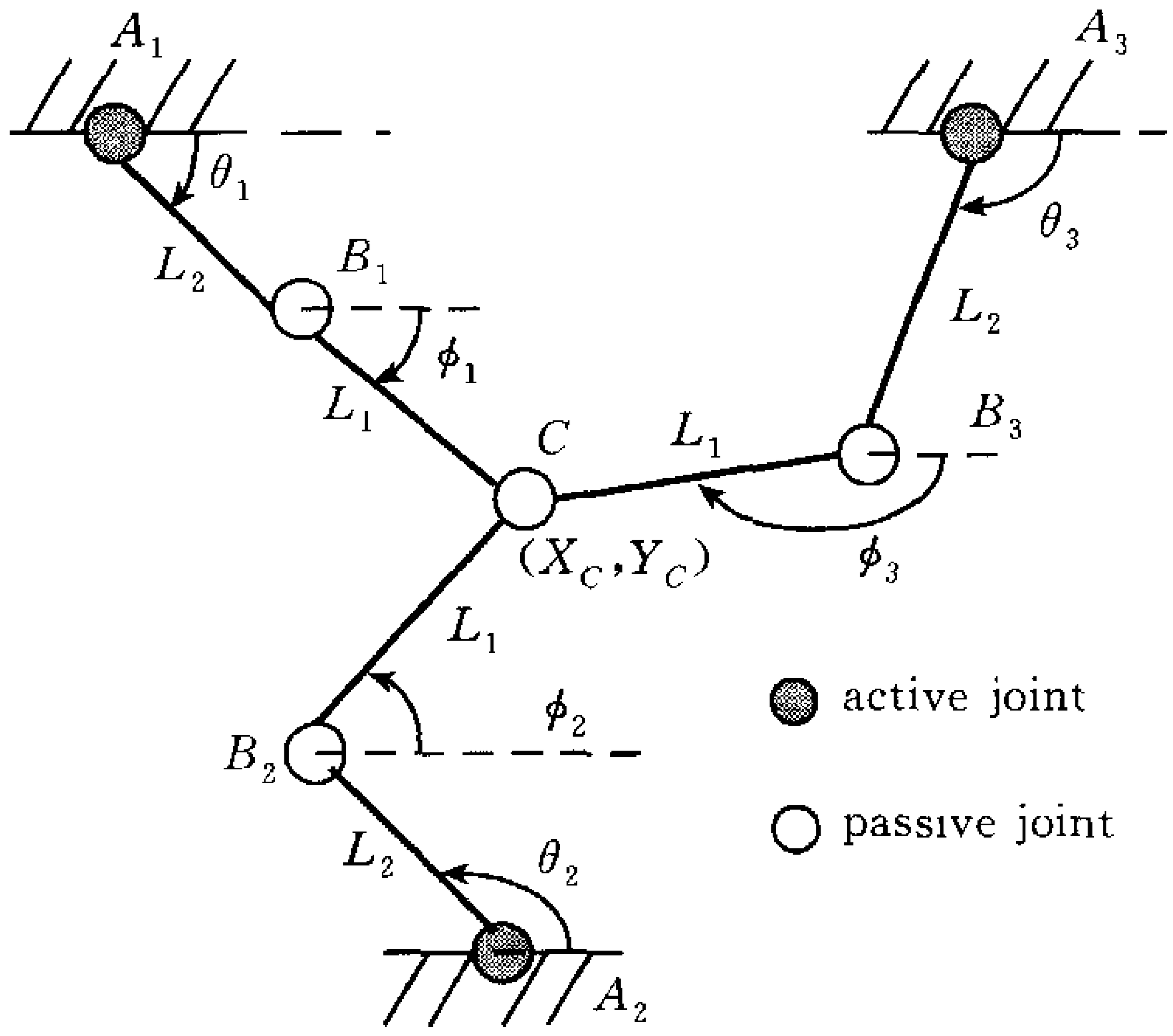

Fig. 2 The planar two-degree-of-freedom parallel manipulator

5 Simulation

Assume the desired constraint forces $\boldsymbol{f}_d = 0$ and the desired motion trajectory described by $\theta_{1d} = 1 + 0.2\sin(5t)$ and $\theta_{2d} = 2 + 0.2\sin(8t)$. The sampling interval of the controller is taken as 10ms. For validating the robustness of the control algorithm we add 10% error in the inertia matrix and quality of each staff. Figure 3 is the tracking results of the joint θ_1 in Cartesian space. Figure 4 shows the tracking results of the constraint force. These results show that both position tracking error and force error are small, and the stability of the controller is satisfactory.

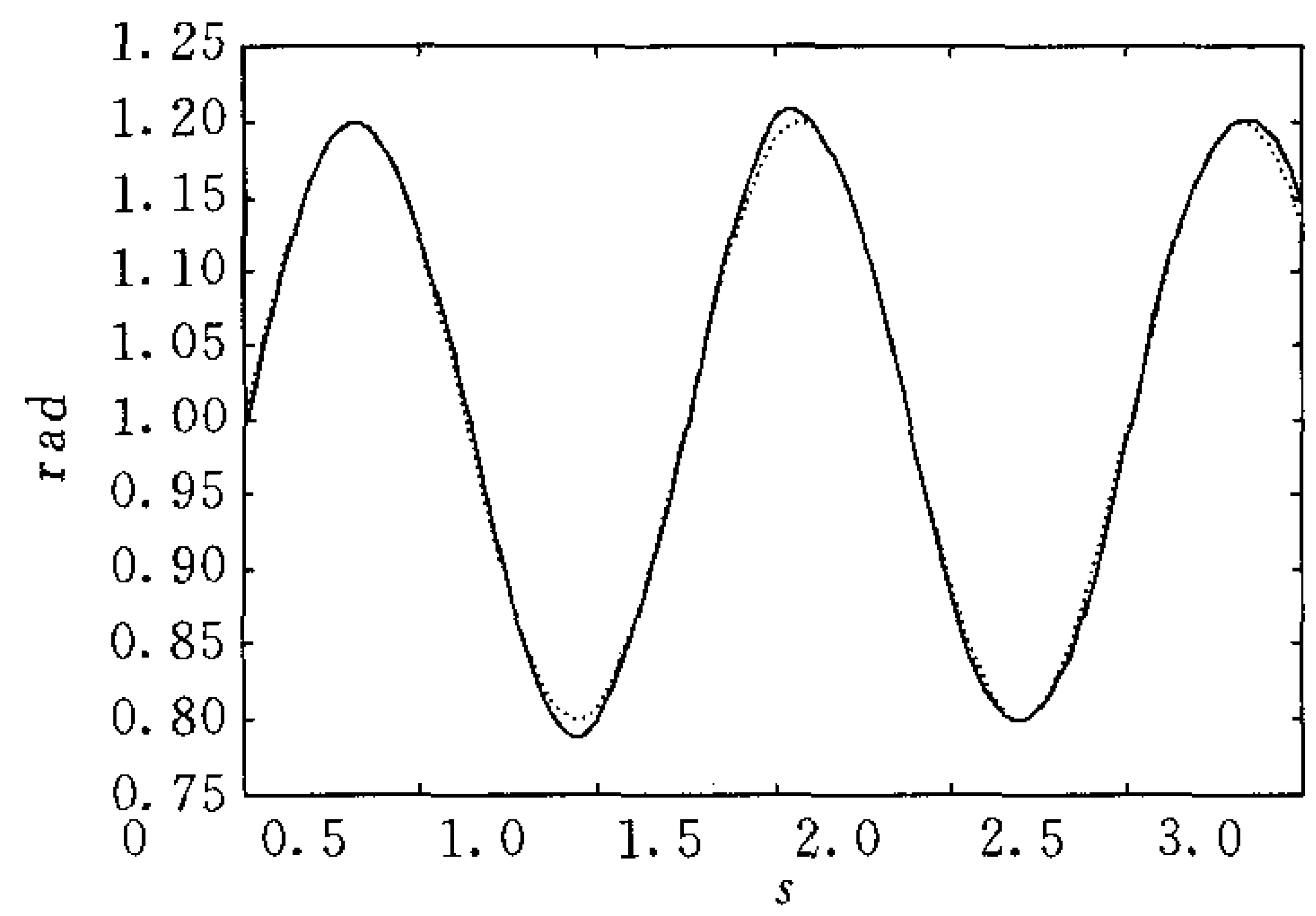

Fig. 3 Tracking results of joint θ_1
(Dotted line: desired values; real line: measure values)

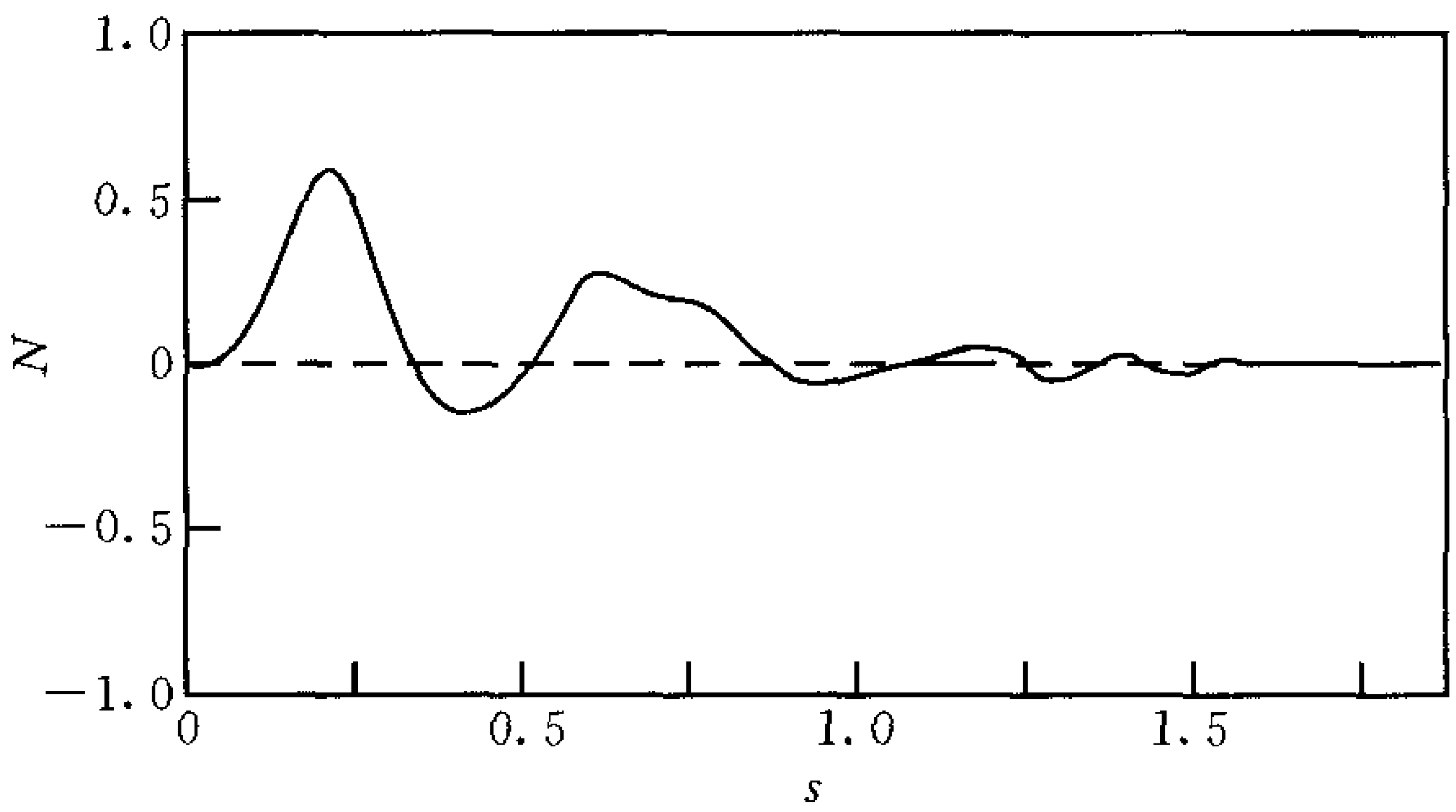

Fig. 4 Tracking results of constraint forces

6 Conclusions

In this paper we decoupled the inverse dynamics of parallel manipulators into position space and constraint force space based on the geometric properties of constraint submanifold. A nonlinear adaptive hybrid position/force control algorithm has been proposed for the planar two-degree-of-freedom parallel manipulator. We have also realized minimal joint torque position control on the manipulator. The simulation results have validated the effectiveness of the control algorithm proposed.

References

1 Richard M, Li Z X, Sastry S S. A Methematical Introduction to Robotic Manipulation. Florida: CRC Press, 1994

2 Yoshikawa T. Dynamic hybrid position/force control of robot manipulators——description of hand constrains and calculation of joint driving force. *IEEE Journal of Robotics and Automation*, 1987, **RA-3**(5):321～328

3 McClaroch N H, Wang D W. Feedback stabilization and tracking of contrained robots. *IEEE Transations on Automatic Control*, 1988, **33**(5): 419～426

4 Selig J M. Curvature in force/position control. In Proceedings of IEEE International Conference on Robotics and Automation, Leuven, Belgium, 1998. 1761～1766

5 Shen H, Wu X Z, Li S Y. *Journal of National University of Defense Technology*, 2002, **24**(2): 91～94 (in Chinese)

6 Liu G F, Wu Y L, Wu X Z. Analysis and control of redundant parallel manipulators. In: International Conference on Robotics and Automation, Seoul, Korea, 2001. 3748～3754

7 Han Y, Liu L, Lingarkar R. Adaptive control of constrained robotic manipulators. *International Journal of Robotics and Automation*, 1991, **7**(2): 50～56

SHEN Hui Received his master degree from National University of Defense Technology in 1997. His research interests include parallel manipulators and robot control.

WU Xue-Zhong Received his master and Ph. D. degrees from National University of Defense Technology in 1995 and 1998, respectively. His research interests include parallel manipulators and mechanisms.

LIU Guan-Feng Receivecd his Ph. D. degree from the Department of Electrical and Electronic Engineering, the Hong Kong University of Science and Technology in 2002. His research interests include parallel robots, multifingered robotic hand, and constrained system control.

LI Ze-Xiang Received his master degree in mathematics and the Ph. D. degree in electrical engineering and computer science from the University of California at Berkeley, in 1985 and 1989, respectively. His research interests include robotics, nonlinear system theory, and manufacturing.

冗余驱动并联机械手的混合位置/力自适应控制

沈 辉[1] 吴学忠[1] 刘冠峰[2] 李泽湘[2]

[1](国防科技大学机电工程与自动化学院 长沙 410073)

[2](香港科技大学电气工程学系 香港)

(E-mail: manifold_nudt@163.com)

摘 要 针对冗余驱动并联机构研究一种自适应的混合位置/力控制算法.基于并联机构中约束子流形的几何性质,将冗余驱动并联机构的逆动力学自然投影到位形空间和约束力空间.基于投影方程,提出一种统一的具有渐进稳定性的自适应混合位置/力控制算法.采用最小二范数准则求解冗余解问题,实现了实际驱动关节力矩的优化.仿真结果验证了控制方法的有效性.

关键词 冗余驱动,并联机器人,自适应控制,混合控制

中图分类号 TH112